

## Future Perspectives for Higgs Physics

---

**Sven Heinemeyer<sup>a,\*</sup>**

<sup>a</sup>*Instituto de Física Teórica (UAM/CSIC),  
Universidad Autónoma de Madrid, Cantoblanco, 28049, Madrid, Spain*

*E-mail:* [Sven.Heinemeyer@cern.ch](mailto:Sven.Heinemeyer@cern.ch)

Future perspectives for Higgs physics are outlined. First it is shown that the discovered Higgs boson cannot be the Standard Model Higgs boson, motivating the investigations of Higgs sectors beyond the Standard Model. The secure future, the HL-LHC, and the agreed upon future, an  $e^+e^-$  collider, are briefly discussed. The importance of theory calculations for the full exploitation of the (anticipated) experimental data is emphasized. Finally, the complementarity of collider based Higgs physics and other types of experiments, such as gravitational wave observatories is briefly outlined.

*41st International Conference on High Energy physics - ICHEP2022  
6-13 July, 2022  
Bologna, Italy*

*IFT-UAM/CSIC-22-143*

---

\*Speaker

## 1. Why the Higgs is not the SM Higgs

The discovery of a Higgs boson at ATLAS and CMS in 2012, nearly 50 years after its prediction, was a milestone in high-energy physics [1, 2]. Within theoretical and experimental uncertainties this new particle is consistent with the existence of a Standard-Model (SM) Higgs boson at a mass of  $\sim 125$  GeV [3]. While no sign of Beyond Standard-Model (BSM) physics was (yet) discovered at the LHC, the measurements of Higgs-boson production and decay rates, which are known experimentally to a precision of roughly  $\sim 10 - 20\%$ , leave ample room for BSM interpretations. Consequently, one of the main tasks of the current and future LHC runs, as well as experiments beyond the LHC is to determine whether this particle,  $h_{125}$ , forms part of the Higgs sector of an extended model.

From the theory side this situation is clearer. There are unambiguous data that tell us that the SM cannot be the ultimate theory. The most compelling ones are:

1. gravity is not included in the SM
2. the hierarchy problem (the stability of the Higgs-boson mass w.r.t. quantum corrections)
3. no unification of the three forces in the SM
4. Dark Matter is not included in the SM
5. the Baryon Asymmetry of the Universe (BAU) cannot be explained in the SM
6. neutrino masses are not included in the SM
7. some experimental data are not described correctly within the SM  
( $(g - 2)_\mu$ , flavor anomalies, ...)

This clearly indicates that we have to extend the SM, and thus that the Higgs boson discovered at the LHC cannot be the SM Higgs boson. However, the really important question is

**Q:** does the BSM physics that undoubtedly exists has any (relevant) impact on the Higgs sector?

The two obvious ways to answer this question are

**A<sub>1</sub>:** measure the characteristics of the  $h_{125}$  with highest precision,

**A<sub>2</sub>:** search for additional Higgs bosons (*above* and *below* 125 GeV),

together with a possibly less obvious way

**A<sub>3</sub>:** test “other predictions” of the BSM Higgs sector(s).

In these proceedings we will briefly discuss these future perspectives for Higgs-boson physics.

## 2. The secure future: HL-LHC

The high luminosity stage of the LHC, the HL-LHC, is approved and expected to collect up to  $3 \text{ ab}^{-1}$ , each in ATLAS and in CMS, i.e. about 20 times more integrated luminosity than collected so far. This will allow to measure the properties of the  $h_{125}$  with a much higher precision as compared

to the current accuracy, as well as to extend substantially the reach for new BSM Higgs bosons. Here we just list three prominent examples in these directions.

The  $\kappa$  framework [4] was devised after the Higgs-boson discovery to test the experimental data on Higgs-boson rate measurements at the LHC for deviations from the SM.<sup>1</sup> Effectively, each  $\kappa_p$  parametrizes multiplicatively the deviation of the coupling of the particle  $p$  with the Higgs-boson. The expected deviations of the Higgs couplings from the SM limit depend on the mass scale of the new physics. In general Two Higgs Doublet Model (2HDM)-type models (including the case of the Minimal Supersymmetric Standard Model (MSSM)) one expects deviations from the SM predictions of roughly the following size for the different couplings (here for Yukawa type II) [7],

$$\kappa_V \approx 1 - 0.3\% \left( \frac{200 \text{ GeV}}{M_A} \right)^4, \quad \kappa_t = \kappa_c \approx 1 - 1.7\% \left( \frac{200 \text{ GeV}}{M_A} \right)^2, \quad \kappa_b = \kappa_\tau \approx 1 + 40\% \left( \frac{200 \text{ GeV}}{M_A} \right)^2. \quad (1)$$

Here  $\kappa_{V,t,c,b,\tau}$  denotes the scale factors for the couplings to massive SM gauge bosons, top, charm and bottom quarks and to  $\tau$  leptons, respectively, and  $M_A$  denotes the BSM Higgs-boson mass scale. In composite Higgs models one typically expects effects of [8]

$$\kappa_V \approx 1 - 3\% \left( \frac{1 \text{ TeV}}{f} \right)^2, \quad \kappa_F \approx 1 - (3-9)\% \left( \frac{1 \text{ TeV}}{f} \right)^2, \quad (2)$$

where  $\kappa_F$  is a generic scale factor for the couplings to all fermions, and  $f$  is the compositeness scale. It can be seen that, depending on the scale of new physics (in this case  $M_A$  or  $f$ ) deviations in the sub-percent range for the couplings to gauge-bosons can be expected. For the couplings to fermions, depending on the type and the concrete model, deviations in the per-cent range could be realized.

In Fig. 1 the accuracies of various  $\kappa$ 's expected to be reached at the HL-LHC are shown [9]. The left plot depicts the relative uncertainties for ATLAS (blue/gray) and CMS (red/gray), where blue/red indicates the combined experimental uncertainty, and gray shows the inclusion of theory uncertainties. The right plot demonstrates the ATLAS/CMS combined result with the statistical (systematical) uncertainties indicated in blue (green), the theory uncertainties in red, and the combined result in gray. Here it should be kept in mind that in order to extract absolute values in the  $\kappa$  framework at the (HL-)LHC some theory assumptions must be made. From Fig. 1 it can be seen that many  $\kappa$ 's will be known at the  $\sim 2\%$  level, with  $\sim 4\%$  uncertainties for  $\kappa_{t,b,\mu}$  and  $\sim 10\%$  uncertainty for  $\kappa_{Z\gamma}$ . While this constitutes an important improvement over the current result, it may not be sufficient to reach the sensitivity to new physics scales as indicated in Eqs. (1) and (2).

In Fig. 2 the expected relative precision for the SM Higgs self-coupling,  $\kappa_\lambda := \lambda_{hhh}/\lambda_{\text{SM}}$  is shown [9]. The right plot demonstrates the precisions for the various final states analyzed (ATLAS in blue, CMS in red, the combination in black, and the pure statistical uncertainty in gray). The left plot shows the  $\chi^2$  results for the various final states (in color) and for the combined result in black. At the HL-LHC a  $\sim 50\%$  precision for  $\kappa_\lambda$  can be expected (if the SM value  $\kappa_\lambda = 1$  is realized). While this shows at the  $\sim 2\sigma$  level that  $\kappa_\lambda \neq 0$ , it does not correspond to a precision measurement of this quantity.

<sup>1</sup>Over the last  $\sim 10$  years more refined methods have been developed, in particular the SMEFT framework, see e.g. Refs. [5, 6] and references therein.

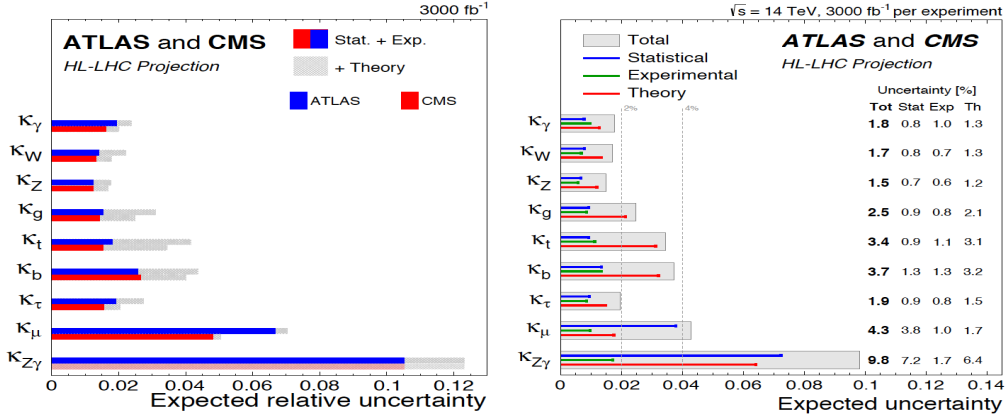


**Figure 1:** Anticipated improvements at the HL-LHC in the precision of  $\kappa$  measurements [9]. Left: expected uncertainty for ATLAS and CMS; right: combined uncertainty (see text).

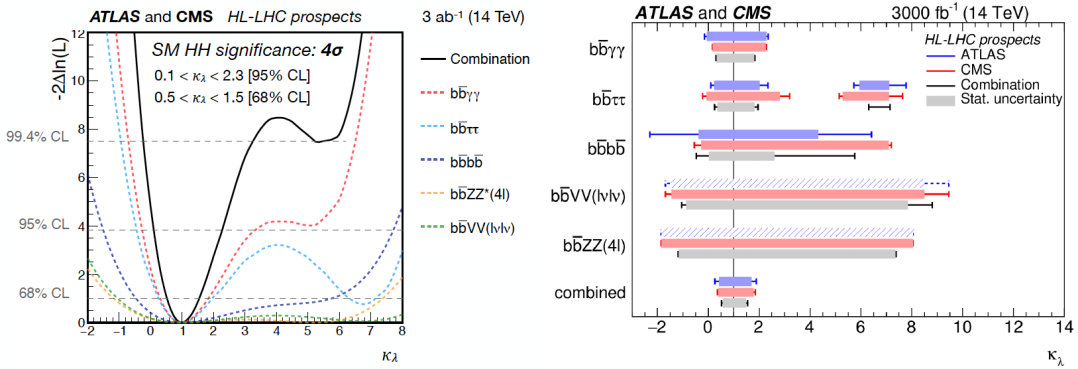


**Figure 2:** Anticipated improvements at the HL-LHC in the precision of  $\kappa_\lambda$  measurements [9] (see text).

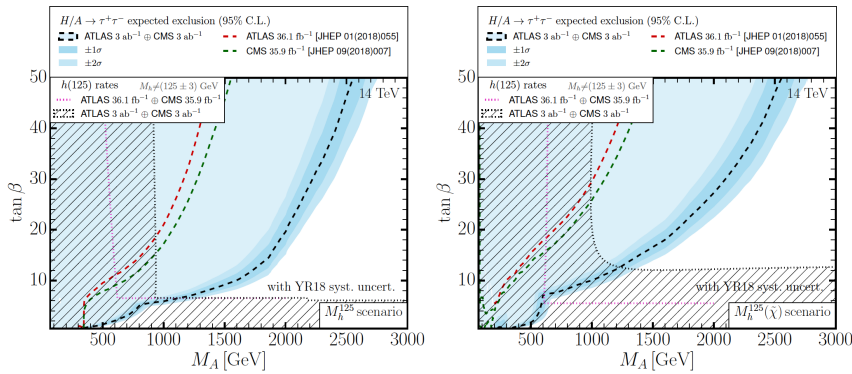


**Figure 3:** Anticipated reach of the HL-LHC in the search for heavy MSSM Higgs bosons [10] (see text).

In Fig. 3 we turn to the anticipated projections for the HL-LHC reach for heavy MSSM Higgs bosons in the  $\tau\tau$  decay channel [10] in the  $M_A$ - $\tan\beta$  plane (where  $M_A$  is the  $C\mathcal{P}$ -odd Higgs boson mass and  $\tan\beta := v_2/v_1$  is the ratio of the two vacuum expectation values). The left (right) plot shows the results in the  $M_h^{125}$  ( $M_h^{125}(\tilde{\chi})$ ) benchmark scenario, see Ref. [11] for details. The (then) current limits are shown in red (green) dashed for ATLAS (CMS), based on the first year

Run 2 data. The pink dotted line indicates the limits from  $h_{125}$  rate measurements. The HL-LHC expectations are shown in black dashed for the Higgs boson searches and in black dotted for the  $h_{125}$  measurements. In both scenarios the BSM Higgs-boson mass scale can be tested up to  $\sim 1.2$  TeV. On the other hand, values of  $M_A \gtrsim 2.5$  TeV remain completely out of reach.

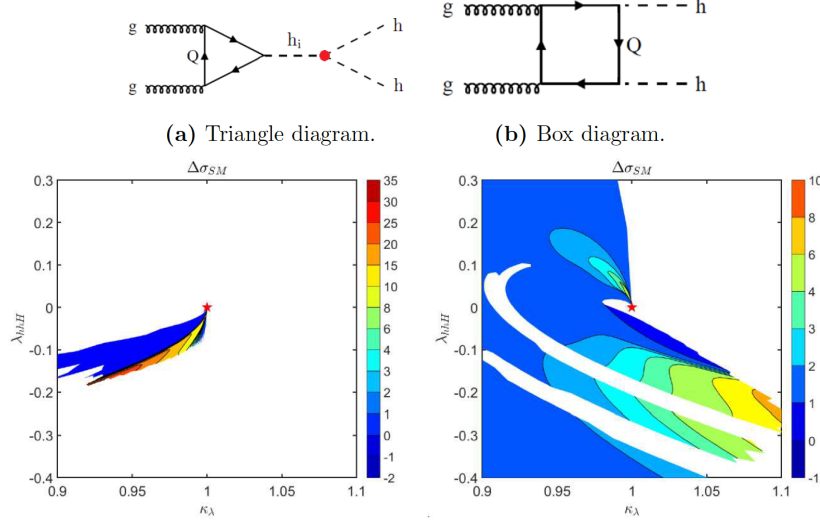


**Figure 4:** Upper part: Feynman diagrams contributing to  $gg \rightarrow hh$  in the 2HDM ( $h_i = h, H$ ). Lower part: di-Higgs production cross section in a selected benchmark plane (see text) in terms of  $\Delta\sigma_{SM} \sim 38 \text{ fb}/4.5$  (see text), taken from Ref. [12].

Finally, in Fig. 4 [12] we demonstrate that the HL-LHC may also have access to triple Higgs couplings (THCs) that involve BSM Higgs bosons. In Ref. [12] the di-Higgs production cross section  $gg \rightarrow hh$  is evaluated in the 2HDM using an accordingly modified version of the code HPAIR [13, 14], where the  $h$  is the  $h_{125}$ . The upper line of Fig. 4 shows the contributing diagrams. The left diagram depicts contributions with a top triangle and  $h, H$  in the  $s$ -channel, where  $H$  is the heavy  $C\mathcal{P}$ -even Higgs boson. These diagrams involve the THCs  $\lambda_{hhh}$  and  $\lambda_{hhH}$ , respectively. The right diagram depicts the (continuum) top-box contribution. The lower row of Fig. 4 presents the results for the di-Higgs cross section in a 2HDM Yukawa type I benchmark plane [15] (with  $\tan\beta = 10$ , all heavy Higgs-boson masses are equal, and  $m_{12}^2 = M_H^2 \cos^2\alpha / \tan\beta$ , with  $\cos(\beta - \alpha)$  and  $M_H$  as free parameters). The results are projected into the  $\kappa_\lambda$ - $\lambda_{hhH}$  plane for  $c_{\beta-\alpha}$  negative (positive) in the left (right) plot. The color coding indicates by how many standard deviations,  $\Delta\sigma_{SM}$ , the 2HDM cross section differs from the SM cross section. For  $\Delta\sigma_{SM}$  the precision expected for  $\kappa_\lambda = 1$  has been used,  $\Delta\sigma_{SM} = 38 \text{ fb}/4.5$  (with  $\sigma(gg \rightarrow hh)_{SM} = 38 \text{ fb}$  at NLO, which can be “seen” at the  $4.5\sigma$  level). The color coding indicates that a non-zero value of  $\lambda_{hhH}$ , but  $\kappa_\lambda \approx 1$  can lead to a sizable enhancement of the cross section in the 2HDM via the resonant enhancement of the  $H$ -exchange diagram. This indicates that the HL-LHC may also have access to BSM THCs (see Ref. [12] for details).

### 3. The agreed upon future: $e^+e^-$ collider(s)

In the high-energy physics community there is a large consensus that the next large experiment following the LHC should be an  $e^+e^-$  collider [16]. As an example, the final text of the European

Strategy for Particle Physics Update [17] states: “. . . there are compelling scientific arguments for a new electron-positron collider operating as a ‘Higgs factory’. Such a collider would produce copious Higgs bosons in a very clean environment, [and] would make dramatic progress in mapping the diverse interactions of the Higgs boson with other particles . . .” The four most advanced proposals are the “International Linear Collider” (ILC) [18], the “Compact Linear Collider” (CLIC) [19], the “Future Circular ( $e^+e^-$ ) Collider” (FCC-ee) [20], and the “Circular  $e^+e^-$  Collider”) (CEPC) [21]. The projected final energy stages are 1 TeV, 3 TeV, 365 GeV and 360 GeV, respectively.



**Figure 5:** Projected precision in  $\kappa_Z$  and  $\kappa_b$  for various future colliders [22].

In Fig. 5 [22] we review the anticipated precision of  $\kappa_Z$  and  $\kappa_b$  for various future collider options, where the ILC (CLIC, FCC-ee, CEPC) projections are shown in green (burgundy, blue, beige). One can observe that w.r.t. the HL-LHC projections (gray, where  $|\kappa_V| < 1$  had to be assumed for a converging fit) a strong improvement can be observed. All four  $e^+e^-$  collider options very roughly yield the same level of precision. Only with this kind of improvement the precision required by Eqs. (1) and (2) can be reached. As a concrete example we show in Fig. 6 the indirect  $2\sigma$  constraints in the  $M_A$ - $\tan\beta$  plane of the  $M_{h,\text{EFT}}^{125}(\tilde{\chi})$  MSSM benchmark scenario from prospective  $h_{125}$  signal-rate measurements at the HL-LHC and the ILC [10], where the point  $M_A = 1$  TeV and  $\tan\beta = 3$  had been assumed to be realized. The light pink area shows the constraints using the projected HL-LHC precision in the  $h_{125}$  couplings. It can be observed that no upper limit on  $M_A$  can be set. This changes once the ILC precision is assumed with the ILC250 (ILC500) ranges shown in medium (dark) pink. In this case an upper limit on the so far unobserved new Higgs-boson mass scale of  $\sim 2100$  GeV ( $\sim 1600$  GeV) can be obtained. This sets a clear target for direct searches at future colliders.

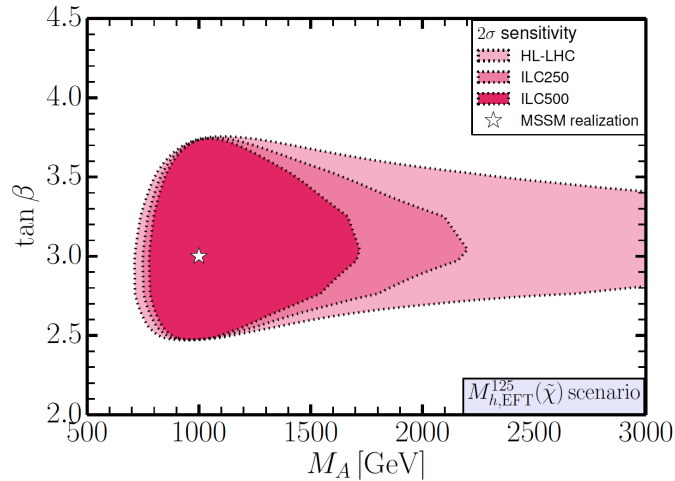


**Figure 6:** Indirect  $2\sigma$  constraints in the  $M_A$ - $\tan\beta$  plane of the  $M_{h,\text{EFT}}^{125}(\tilde{\chi})$  scenario from prospective Higgs-boson signal-rate measurements at the HL-LHC and the ILC [10] (see text).

Finally, in Fig. 7 we show the projections for the precision at the 68% CL on  $\kappa_\lambda$  ( $\kappa_3$  in the plot) obtainable at various future collider options [22]. The light bars indicate the precision using single Higgs production, where  $\lambda_{hhh}$  enters only at the loop level, a method on which circular  $e^+e^-$  colliders must rely, as their center-of-mass energy does not reach the di-Higgs production threshold. The dark colors indicate the precision based on di-Higgs production, which can be obtained at the linear collider options. One can observe that the determination via di-Higgs productions leads to substantially better sensitivities, going down to the level of  $\sim 10\%$  at the ILC1000 and CLIC3000, a factor of  $\sim 5$  improvement w.r.t. the HL-LHC expectations. This will allow to probe the Higgs potential in the SM, but also in BSM models (for the 2HDM see, e.g., Ref. [23], where also an analysis of the sensitivity to  $\lambda_{hhH}$  can be found). Here it should be kept in mind that the results in Fig. 7 assume  $\kappa_\lambda = 1$ , and the accuracies can change substantially for other values, see below.

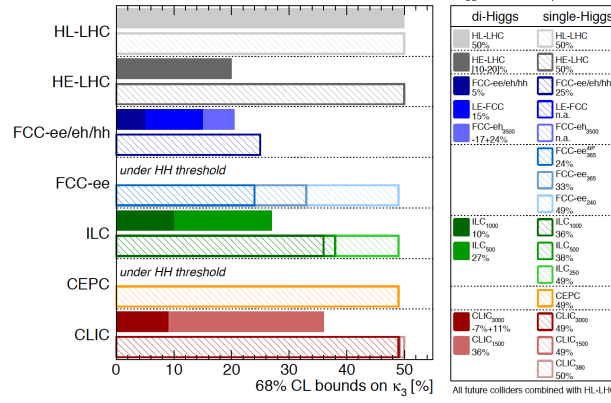


**Figure 7:** Sensitivity at the 68% CL on  $\kappa_\lambda$  at various future colliders [22].

A second main task of a future  $e^+e^-$  collider, besides the precision measurement of the  $h_{125}$ , is the search for new Higgs bosons, which would clearly indicate a BSM Higgs sector. In models which extend the SM by doublets and singlets, the production of two BSM Higgs bosons together is favored over the single production. Owing to other theoretical and experimental constraints, this limits the discovery reach of an  $e^+e^-$  collider to roughly  $M_H \lesssim \sqrt{s}/2$  (where  $M_H$  represents generically the BSM Higgs mass scale). This substantially limits the discovery reach of circular machines for masses above 125 GeV, whereas linear machines, depending on their final energy stage, have a unique discovery potential. The situation is different for BSM Higgs bosons below 125 GeV. Here all future  $e^+e^-$  collider proposals possess an important coverage for a discovery and/or (subsequent) precision measurements.

As a (toy) example, based on recent excesses observed in the Higgs search data, we will briefly discuss one above and one below 125 GeV. The first one was seen by CMS in the  $t\bar{t}$  final state at  $\sim 3\sigma$  at a mass scale of  $\sim 400$  GeV [24]. It was best interpreted as a  $CP$ -odd Higgs boson produced in gluon fusion,  $gg \rightarrow A \rightarrow t\bar{t}$ , with  $\Gamma_A/M_A$  in the range of a few percent and a coupling strength relative to an SM-like Higgs between  $\sim 0.5$  and  $\sim 0.9$ . It was shown in Ref. [25] that this excess can be well described by a  $CP$ -odd Higgs boson in the Next-to-2HDM (N2HDM, where the 2HDM is extended by a real singlet) or the Next-to-MSSM (NMSSM, where the MSSM is extended by a complex singlet). Interestingly, the indicated mass scale of  $\sim 400$  GeV would allow the production of this particle at the ILC1000, or at CLIC1500 (or higher). The second excess was seen at  $\sim 96$  GeV in the di-photon final state at  $\sim 3\sigma$  at CMS [26] and in the  $b\bar{b}$  final state

at  $\sim 2\sigma$  at LEP [27]. Such a state could be produced (depending on its couplings to  $Z$  bosons) in large quantities at any future  $e^+e^-$  collider operating at LEP energies, or higher. In the left plot of Fig. 8 [25] the  $M_A$ - $c_{A\bar{t}t}$  plane is shown, where  $c_{A\bar{t}t}$  is the coupling strength of the  $C\mathcal{P}$ -odd Higgs to top quarks relative to an SM-like Higgs. The expected exclusion line (black dashed) together with its 1 and  $2\sigma$  uncertainties, as well as the observed exclusion in light blue are taken from Ref. [24]. The colored points demonstrate where the N2HDM can describe both excesses together, or where the NMSSM can describe the 400 GeV excess (and possibly the di-photon excess at CMS, but not the LEP excess), with the color coding indicating  $\Gamma_A/M_A$ .

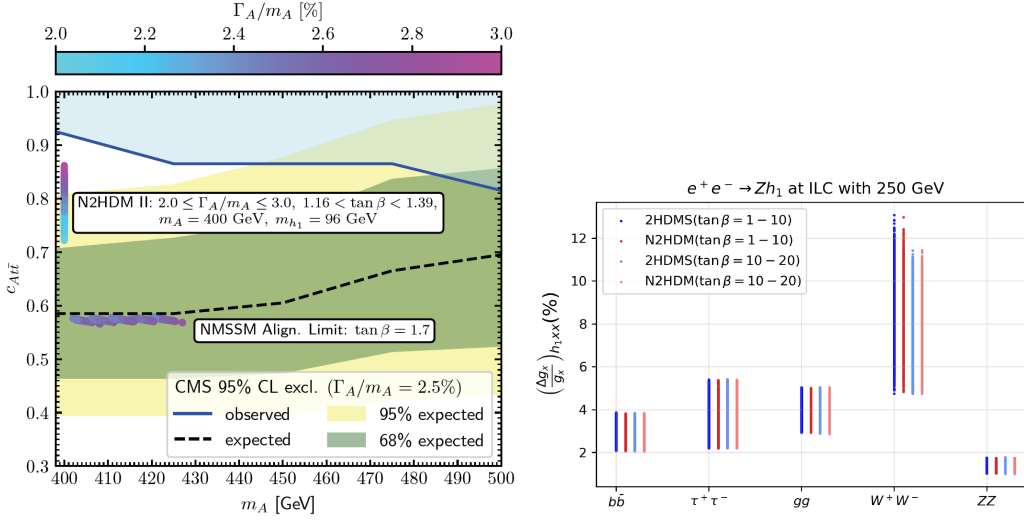


**Figure 8:** Left:  $M_A$ - $c_{A\bar{t}t}$  plane in the N2HDM and NMSSM; color coding indicates  $\Gamma_A/M_A$  and where the 400 GeV and 96 GeV excesses can be realized [25] (see text). Right: anticipated coupling precision of  $h_{96}$  in the N2HDM and 2HDMS at the ILC250 [28] (see text).

Interpreting the excesses in concrete models allows to make clear predictions for current and future collider searches and measurements. As discussed above, the  $h_{96}$  can be produced at the first stages of any of the future  $e^+e^-$  colliders. Taking the ILC250 as a concrete example, in Ref. [28] it was analyzed to which precision the couplings of the  $h_{96}$  can be measured. The measurement of the  $h_{96}ZZ$  couplings proceeds directly via the Higgs-Strahlung production mode,  $e^+e^- \rightarrow Zh_{96}$ , with  $Z \rightarrow e^+e^-, \mu^+\mu^-$ . The other coupling measurements rely on the subsequent decay of the  $h_{96}$  to the respective final state. As underlying models the N2HDM as well as the 2HDMS (the 2HDM plus a complex singlet), both of Yukawa type II, were assumed. The anticipated precisions in the various  $h_{96}$  couplings can be seen in the right plot of Fig. 8 [28], where the color coding distinguishes the two models, as well as two intervals for  $\tan \beta$ . It can be observed that the coupling to  $Z$  bosons can be determined at the 1% level, the couplings to  $b\bar{b}$ ,  $\tau^+\tau^-$ ,  $g\bar{g}$  at the level of 2–5%, and the coupling to  $W^+W^-$  between 5% and 12%. This demonstrates that a future  $e^+e^-$  collider can not only search and find new (light) Higgs bosons, but can also perform an accurate analysis of its couplings. This in turn will allow to determine the underlying parameter space with high precision.



#### 4. Theory meets Experiment

The discovery of a Higgs boson at the LHC required an enormous experimental effort, and the LHC provided (and continues to provide) a wealth of experimental data. However, the experimental data can only fully be exploited if it is compared to theory predictions at the same level of accuracy.<sup>2</sup> The non-background like events seen at the LHC in the first  $\sim 6 \text{ fb}^{-1}$  of Run 1 data (plus the 7 TeV data) could be interpreted as the discovery of a Higgs boson only by comparison to the corresponding theory predictions. In order to provide these theory predictions in the year 2010, i.e. two years prior to the Higgs-boson discovery, the LHC Higgs Cross Section Working Group (now LHC Higgs Working Group, LHCHWG) was founded [29]. Its task was (and is) to provide theory predictions that match the (anticipated) experimental accuracies in the search for Higgs bosons, as well as in the interpretation of the (now discovered) signal. A related task was (and is) to develop strategies for the extraction of experimental data on an observed Higgs boson. As an example, the  $\kappa$  framework [4] was devised in 2012 to obtain information on the Higgs-boson couplings to SM particles, see Sect. 2. The LHCHWG, composed jointly out of theorists and experimentalists, continues to play a crucial role in the interpretation of the observed signal at the LHC, as well as in the search for new BSM Higgs bosons.

The exploration of the  $h_{125}$  at future  $e^+e^-$  colliders will require an enormous improvement in the theoretical predictions to meet the anticipated high experimental accuracy (see, e.g., Ref. [30]). The need for a coordinated effort to match the expected experimental precision at an  $e^+e^-$  collider is at least as high, if not higher, as it was for the LHC. Therefore, the theory effort should always be seen as an integral part of any (future) Higgs (or SM/BSM) physics program.

#### 5. Complementarity

One intriguing scenario for the future is the possible complementarity and synergy of collider based Higgs physics with gravitational wave (GW) experiments. One prominent example for the realization of BAU is baryogenesis, which requires a strong first-order electroweak phase transition (FOEWPT) in the early universe, which can take place when the vacuum goes from a symmetric phase to the broken phase: the universe cools down and forms a second minimum in the Higgs potential away from the origin. At the critical temperature  $T_c$  both minima have the same energy value and should be separated by a barrier (otherwise a second order phase transition or a smooth cross over can take place). The universe then further cools down and at the nucleation temperature  $T_n$  it tunnels through the barrier from the symmetric phase to the broken phase, the EW minimum with a vev of  $\sim 246 \text{ GeV}$ . This in turn generates GWs that could be detectable with GW observatories such as the (approved) LISA [31, 32].

In the SM this is not possible with the measured Higgs-boson mass of  $\sim 125 \text{ GeV}$ . In BSM Higgs sectors with additional degrees of freedom, however, this constitutes a realistic possibility. As an example we show in Fig. 9 [33] a parameter plane in the 2HDM type II with  $M_h = 125 \text{ GeV}$ ,  $\tan \beta = 3$ ,  $\cos(\beta - \alpha) = 0$ ,  $m_{12}^2 = M_H^2 \sin \beta \cos \beta$ , and with  $M_A = M_{H^\pm}$  and  $M_H$  as free parameters. In the benchmark plane various zones (A-F) can be distinguished by their thermal history of the

<sup>2</sup> The full uncertainty of a measured quantity is given by the (linear) sum of the experimental and theoretical uncertainties.

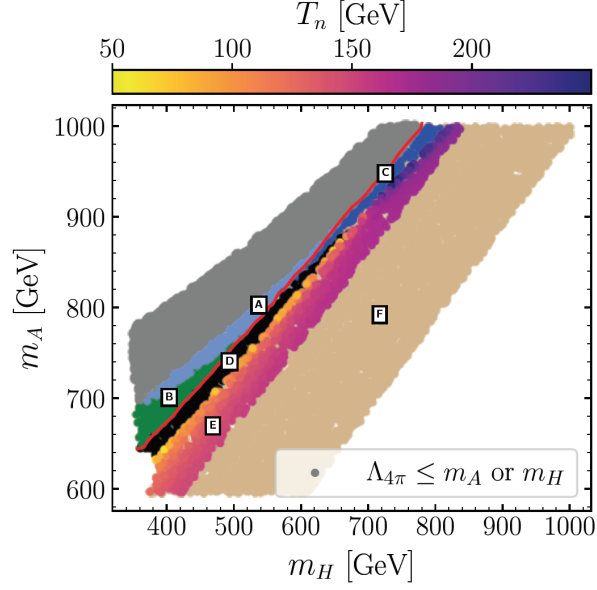


**Figure 9:** Thermal history of a 2HDM type II scan [33] in the  $M_H$ - $M_A$  plane. The color coding indicates the nucleation temperature  $T_n$  (in zone E, see text).

universe. In zone E the above discussed FOEWPT takes place, with the color coding indicating  $T_n$ , where lower  $T_n$  yields a stronger GW signal. Here it is interesting to observe that the parameter space with the potentially largest GW signal, located in zone D shown in black, features “vacuum trapping”: the broken phase is the deepest minimum, but the barrier between the symmetric phase and the EW minimum is so strong that no transition takes place. On the other hand, if zone E is realized in nature and the GW signal is sufficiently strong (to be detected by LISA or other possible future GW observatories) the collider experiments for BSM Higgs sectors and the GW detectors yield complementary information about the BSM Higgs sector.

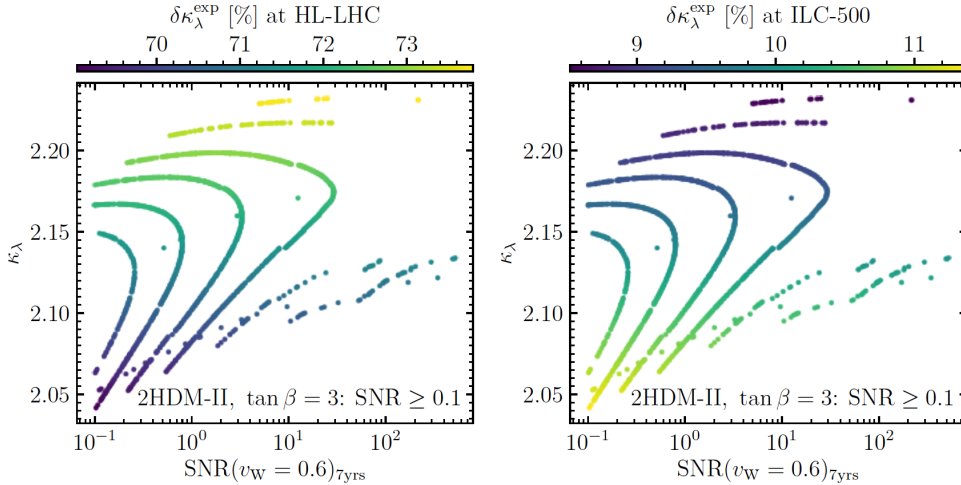


**Figure 10:** Parameter points from a 2HDM type II scan [33] in the LISA SNR- $\kappa_\lambda$  plane (see text). The color code indicates the precision  $\delta\kappa_\lambda^{\text{exp}}$  at the HL-LHC (left) and the ILC500 (right).

As a final step in this analysis we show in Fig. 10 [33] the parameter space of the previous

benchmark plane that yields a signal-to-noise ratio (SNR) at LISA larger than 0.1, as shown in the horizontal axis (using 7 years of data taking and a bubble wall velocity of  $v_W = 0.6$ ). An observable signal will likely require an SNR larger than 1. It is found that in this area the higher-order corrections to  $\lambda_{hhh}$  yield values of  $\kappa_\lambda \sim 2$ , i.e. a strong enhancement w.r.t. the SM value, as can be seen in the vertical axis. This is a typical result for FOEWPT in the 2HDM. The color coding in the figure indicates the precision with which the HL-LHC (left plot) and the ILC500 (right plot) can determine  $\kappa_\lambda$ . The anticipated precision changes because of the changed interferences of signal and background diagrams contributing to the di-Higgs production cross sections. One can see in Fig. 10 that the HL-LHC precision worsened substantially w.r.t. the SM, i.e.  $\kappa_\lambda = 1$ , down to  $\sim 72\%$ . On the other hand, the precision at the ILC500 improves by about a factor of  $\sim 2$  w.r.t.  $\kappa_\lambda = 1$ , yielding a determination at the level of  $\sim 10\%$ . The important overall conclusion is that if BAU is generated by baryogenesis, requiring a FOEWPT in the early universe, this likely worsens the prospects to determine  $\lambda_{hhh}$  at the HL-LHC, but substantially improves the ILC500 prospects.

## 6. Main conclusions

After the full exploitation of the HL-LHC Higgs data, let's build an  $e^+e^-$  collider as quickly as possible to study the observed Higgs boson in detail and to search for new Higgs bosons above and below 125 GeV.

## References

- [1] G. Aad *et al.* [ATLAS Collaboration], Phys. Lett. B **716** (2012) 1 [arXiv:1207.7214 [hep-ex]].
- [2] S. Chatrchyan *et al.* [CMS Collaboration], Phys. Lett. B **716** (2012) 30 [arXiv:1207.7235 [hep-ex]].
- [3] G. Aad *et al.* [ATLAS and CMS Collaborations], JHEP **1608** (2016) 045 [arXiv:1606.02266 [hep-ex]].
- [4] S. Heinemeyer *et al.* [LHC Higgs Cross Section Working Group], [arXiv:1307.1347 [hep-ph]].
- [5] D. de Florian *et al.* [LHC Higgs Cross Section Working Group], [arXiv:1610.07922 [hep-ph]].
- [6] G. Passarino and M. Trott, [arXiv:1610.08356 [hep-ph]].
- [7] H. Baer *et al.* [arXiv:1306.6352 [hep-ph]].
- [8] S. Dawson *et al.* [arXiv:1310.8361 [hep-ex]].
- [9] M. Cepeda *et al.* CERN Yellow Rep. Monogr. **7**, 221-584 (2019) [arXiv:1902.00134 [hep-ph]].
- [10] H. Bahl, P. Bechtle, S. Heinemeyer, S. Liebler, T. Stefaniak and G. Weiglein, Eur. Phys. J. C **80** (2020) no.10, 916 [arXiv:2005.14536 [hep-ph]].
- [11] E. Bagnaschi *et al.* Eur. Phys. J. C **79** (2019) no.7, 617 [arXiv:1808.07542 [hep-ph]].
- [12] F. Arco, S. Heinemeher, M. Muhlleitner and K. Radchenko, IFT-UAM/CSIC-22-073.

- [13] H. Abouabid *et al.*, JHEP **09** (2022), 011 [arXiv:2112.12515 [hep-ph]].
- [14] R. Grober, M. Muhlleitner, and M. Spira, Nucl. Phys. B **925** (2017), 1 [arXiv:1705.05314 [hep-ph]].
- [15] F. Arco, S. Heinemeyer and M. J. Herrero, Eur. Phys. J. C **80** (2020) no.9, 884 [arXiv:2005.10576 [hep-ph]].
- [16] See: <https://indico.cern.ch/event/808335/contributions/3365090>.
- [17] See: <http://council.web.cern.ch/council/en/EuropeanStrategy/ESStatement.pdf>.
- [18] See: <http://www.linearcollider.org>.
- [19] See: <https://clic.cern>.
- [20] See <https://home.cern/science/accelerators/future-circular-collider>.
- [21] See <http://cepc.ihep.ac.cn>.
- [22] J. de Blas *et al.*, JHEP **01** (2020), 139 [arXiv:1905.03764 [hep-ph]].
- [23] F. Arco, S. Heinemeyer and M. J. Herrero, Eur. Phys. J. C **81** (2021) no.10, 913 [arXiv:2106.11105 [hep-ph]].
- [24] A. M. Sirunyan *et al.* [CMS], JHEP **04** (2020), 171 [erratum: JHEP **03** (2022), 187] [arXiv:1908.01115 [hep-ex]].
- [25] T. Biekötter, A. Grohsjean, S. Heinemeyer, C. Schwanenberger and G. Weiglein, Eur. Phys. J. C **82** (2022) no.2, 178 [arXiv:2109.01128 [hep-ph]].
- [26] A. M. Sirunyan *et al.* [CMS], Phys. Lett. B **793** (2019), 320-347 [arXiv:1811.08459 [hep-ex]].
- [27] R. Barate *et al.* [LEP Working Group for Higgs boson searches, ALEPH, DELPHI, L3 and OPAL], Phys. Lett. B **565** (2003), 61-75 [arXiv:hep-ex/0306033 [hep-ex]].
- [28] S. Heinemeyer, C. Li, F. Lika, G. Moortgat-Pick and S. Paasch, Phys. Rev. D **106** (2022) no.7, 075003 [arXiv:2112.11958 [hep-ph]].
- [29] See: <https://twiki.cern.ch/twiki/bin/view/LHCPhysics/CrossSections> and <https://twiki.cern.ch/twiki/bin/view/LHCPhysics/LHCHXSWG>.
- [30] S. Heinemeyer, S. Jadach and J. Reuter, Eur. Phys. J. Plus **136** (2021) no.9, 911 [arXiv:2106.11802 [hep-ph]].
- [31] C. Caprini *et al.*, JCAP **03** (2020) 024 [arXiv:1910.13125 [astro-ph.CO]].
- [32] P. Auclair *et al.*, [arXiv:2204.05434 [astro-ph.CO]].
- [33] T. Biekötter, S. Heinemeyer, J. No, O. Olea and G. Weiglein, [arXiv:2208.14466 [hep-ph]].